Microstructure and oxygen evolution of Fe–Ce mixed oxides by redox treatment

Kongzhai Li [a,b], Masaaki Haneda [b], Peihong Ning [a], Hua Wang [a], Masakuni Ozawa [b,c,*]

[a] Engineering Research Center of Metallurgical Energy Conservation and Emission Reduction, Ministry of Education, Kunming University of Science and Technology, Kunming 650093, Yunnan, China
[b] Advanced Ceramics Research Center, Department of Frontier Materials, Nagoya Institute of Technology, Asahigaoka, Tajimi, Gifu 507-0071, Japan
[c] Department of Materials Science and Engineering, EcoTopia Science Institute, Nagoya University, Furo-cho, Chikusa, Nagoya 464-8603, Japan

A R T I C L E I N F O

A B S T R A C T

The relationship between structure and reduction/redox properties of Fe–Ce mixed oxides with a Fe content of 5, 10, 20 or 30 mol%, prepared by a coprecipitation method, were investigated by XRD, Raman, TEM, TPR and TPO techniques. It is found that all the iron ions can be incorporated into the ceria lattice to form a solid solution for the FeCe 5 (Fe 5%) sample, but amorphous or crystal Fe_2O_3 particles were found to be present on the Fe–Ce oxide samples with higher the iron content. The reducibility of single solid solution was much better than the pure CeO_2, and the appearance of dispersed Fe_2O_3 particles improved the surface reducibility of materials. The iron ions incorporated into the CeO_2 lattice accelerated the oxygen release from bulk to surface, and surface Fe_2O_3 particles in close contact to CeO_2 acted as a catalyst for the reaction between solid solution and hydrogen. The microstructure of exposed Fe_2O_3 with Ce–Fe–O solid solution allows the Fe–Ce mixed oxides to own good reducibility and high OSC, which also counteracts the deactivation of the reducibility resulting from the sintering of materials in the redox cycling.

© 2013 Elsevier B.V. All rights reserved.

1. Introduction

CeO_2 is well known as an oxygen buffer in three way catalyst (TWC) due to its outstanding oxygen storage capacity (OSC) [1,2]. Since the OSC of single CeO_2 degrades quickly when suffered thermal treatment due to the significant decrease of the surface area, CeO_2-based mixed oxides were proposed [3]. Introducing metal ions with lower valence (e.g., M^{3+}) or small size (e.g., Zr^{4+}) into ceria lattice to form a solid solution is performed to improve OSC as well as the catalytic activity and stability [4]. Eco-friendly Fe_2O_3 abundance, as well as low cost, makes it particularly attractive and highly competitive as an additive. Furthermore, the synergistic effect of iron and cerium oxides is expected, because Fe_2O_3 is also an excellent OSC material and an important active component in many catalytic oxidation reactions such as hydrocarbon or CO oxidation which is same with the application area of CeO_2 [5–8].

Ce–Fe mixed oxides have been prepared via solution chemistries, including hydrothermal method [4,9], sol–gel method [10,11], microemulsion method [12] and coprecipitation method [13–23]. Numbers of iron ions were successfully incorporated into the ceria lattice, and it is generally accepted that the limited solubility of iron ions can reach to 0.3 as molar fraction of cation [17]. Iron ions doping to ceria based solid solution shows a remarkable enhancement on the textural properties (e.g., BET area or crystallite size) and oxygen storage-release ability due to the strong Fe–O–Ce interaction [9–12,14,16–18,24]. Aneggi et al. [16] proposed that the high degree of Fe–O–Ce interaction was attributed to two reasons: (i) the formation of cubic ceria-based solid solution where the interaction takes place through the sharing of oxygen anion defined by the Fe—O—Ce bonds and (ii) the presence of Fe_2O_3 particles in close contact with ceria where the reactivity of exposed iron site within and in close contact with solid solution can play a significant role in the catalytic behavior. Our previous experiments also indicated that Fe–Ce mixed oxides show good activity for methane partial oxidation [19–21]. These findings suggest that the surface iron oxides in the system of Fe–Ce mixed oxides play an important role to form active lattice oxygen for oxidation catalysis. Also, since the OSC and redox property are very important to the applications in catalysis, an investigation on the effect of structural features of Fe–Ce mixed oxides owns considerable value for the design of novel OSC materials.

In the present work, the relationship between structure and redox properties of Fe–Ce mixed oxides is investigated. Especially, the roles of iron species during the reduction and redox treatments is discussed in detail by using the results of XRD, Raman, TEM, TPR and TPO measurements.

* Corresponding author. Tel.: +81 52 789 5863; fax: +81 52 789 5863.
E-mail address: ozawa@numse.nagoya-u.ac.jp (M. Ozawa).

2. Experimental

2.1. Material preparation

CeO$_2$ and Fe–Ce mixed oxides with a Fe content of 5, 10, 20 or 30 mol% (labeled as FeCe 5, FeCe 10, FeCe 20, FeCe 30, respectively) were prepared by a coprecipitation method. The required amounts of Ce(NH$_4$)$_2$(NO$_3$)$_6$ (Wako, Japan, 95%) and/or Fe(NO$_3$)$_3$·9H$_2$O (Wako, Japan, 99%) were dissolved in distilled water, and then mixed using a magnetic stirrer at room temperature for 30 min. The hydroxides were precipitated by dropping an ammonia 8 wt % aqueous solution (Wako, Japan, 25 wt % diluted to 8 wt % by water). The mixtures were stirred for 3 h, after reaching the pH to 10. The precipitates were dried at 110 °C for 24 h, subjected to decomposition at 600 °C in air for 3 h, and heated at 800 °C for 3 h. The final Ce/Fe ratios in all the prepared samples were measured by using X-ray fluorescence (XRF) technique. It is found that the changes between the final data and starting data are lower than 1% in all cases.

2.2. Physical characterizations

Powder X-ray diffraction (XRD) patterns were recorded using a Rigaku MiniFlex diffractometer with Cu Kα radiation at 40 kV and 40 mA. The X-ray diffractogram was recorded at scanning rate of 1°/min with a 0.02° step size in the 2θ range between 10 and 80°. Raman spectra were measured with a JASCO (Japan) NRS-3100 Raman Spectrometer, equipped with a TE-cooled charge coupled device (CCD) detector and a green laser (λ = 532 nm, frequency-doubled Nd:YVO$_4$, Showa Optronics, Japan), under the ambient atmosphere. The BET surface area was determined by using a volumetric adsorption apparatus by nitrogen adsorption at −196 °C using TriStar 3000 (Micromeritics, USA). The microstructures and morphologies were investigated using a JEOL (Japan) JEM-2100 (UHR) transmission electron microscope (TEM) at 200 keV.

2.3. TPR, TPO and OSC measurements

Temperature-programmed reduction (TPR) and temperature-programmed oxidation (TPO) measurements were performed using BP-1s type apparatus (Henmi, Japan). In TPR, the sample (100 mg) was heated from room temperature to 800 °C (hold at 800 °C for 20 min) in a 30 cm^3 min^{-1} flow of 5% H$_2$/Ar at a heating rate of 10 °C min^{-1}. The consumption of H$_2$ was monitored using a thermal conductivity detector (TCD). After the TPR cycle, the flow was switched to Ar and the sample was cooled down to 600 °C at a cooling rate of 10 °C min^{-1}. Thereafter, O$_2$ pulses were injected on the reduced sample at 600 °C, and the OSC was obtained by calculating the consumption of oxygen in the re-oxidation process. TPO experiments were also performed after the TPR measurements. The flow was switched to Ar with cooling of sample to room temperature (RT), and then the oxidation of the materials was performed from RT to 600 °C at a rate of 10 °C min^{-1}. The TPR/TPO redox process was repeated for three times for each sample.
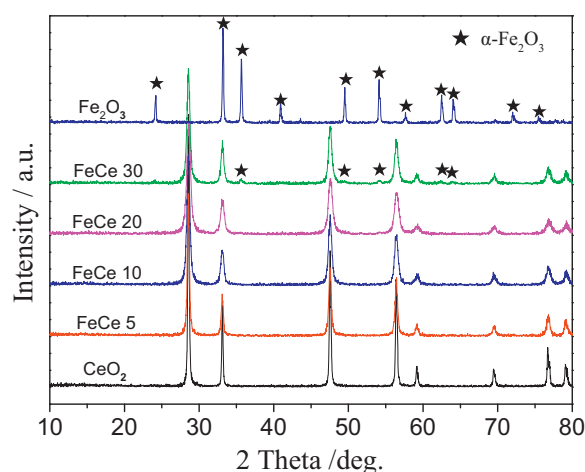

Fig. 1. XRD patterns of CeO$_2$, Fe$_2$O$_3$ and different Fe–Ce mixed oxides.

3. Results and discussion

3.1. Structure of Fe–Ce mixed oxides

Fig. 1 shows the XRD patterns of the prepared Fe–Ce mixed oxide powders. The single CeO$_2$ diffractogram corresponded to a cubic fluorite-structured material (*Fm−3m*) [25] and all the diffraction peaks for pure Fe$_2$O$_3$ was attributed to a hexagonal hematite structure [26]. The diffractograms for all the mixed oxides were similar with that of the single CeO$_2$, showing a fluorite structure. Fe$_2$O$_3$ phase (hematite) can only be detected on the FeCe 30 sample. The lattice constant for ceria slightly decreased with the addition of iron ions (Table 1), evidencing the incorporation of smaller Fe^{3+} into the lattice of CeO$_2$ [4,14]. The crystallize size of CeO$_2$ also decreased due to the addition of Fe$_2$O$_3$ (see Table 1), which suggests that combination of CeO$_2$ and Fe$_2$O$_3$ could strongly inhibit the growth of CeO$_2$ particles under thermal treatment.

Fig. 2 shows the Raman spectra of Fe–Ce oxide samples. The single CeO$_2$ exhibited a prominent band at 466 cm^{-1} corresponding to F$_{2g}$ Raman active mode in metal dioxides with a fluorite-like structure [14]. For the mixed oxides, the main band at around 460 cm^{-1} was also observed, and this band sequentially shifted to lower frequencies with the increase of iron content. The value of the red shift of the Raman band at around 460 cm^{-1} for each mixed oxide sample was shown in Fig. 2(B). In Raman spectra of the fluorite-type oxides, the red shift of ceria band was reported to be associated with the lattice contraction due to the cation doping [4,27]. It should be emphasized that the lattice shrinkage of CeO$_2$ after Fe$_2$O$_3$ doping, observed by XRD measurement, is very limited but the Raman shift of the ceria band is distinct. This phenomenon suggests that the Fe–Ce oxides are not uniform, and the solid solution has higher content of Fe on the surface than that in the bulk of powder. Higher iron contents resulted in wider full width at half maximum (FWHM) of the ceria main band, indicating lower crystallite size of ceria [28]. It should be noted that α-Fe$_2$O$_3$ was detected on the FeCe 10

Table 1
Structural characterization and OSC of CeO$_2$, Fe$_2$O$_3$ and Fe–Ce oxides.

Samples	Phase	Crystallite size of CeO$_2$ ss (nm)	Lattice constant of CeO$_2$ ss (nm)	S_{BET} (m^2 g^{-1})	OSC (mmol/g)
CeO$_2$	–	58.7	0.5412	2.2	0.30
Fe$_2$O$_3$	–	71.1	–	2.7	0.81
FeCe 5	CeO$_2$ ss	28.0	0.5410	1.8	0.50
FeCe 10	CeO$_2$ ss + α-Fe$_2$O$_3$ (by Raman)	18.7	0.5408	1.5	0.78
FeCe 20	CeO$_2$ ss + α-Fe$_2$O$_3$ (by Raman)	14.7	0.5407	2.9	1.08
FeCe 30	CeO$_2$ ss + crystalline α-Fe$_2$O$_3$	18.9	0.5406	7.6	1.33

ss: solid solution; S_{BET}: specific surface area.